Annealing of dry etch damage in metallized and bare (-201) Ga$_2$O$_3$

Jiancheng Yang and Fan Ren
Department of Chemical Engineering, University of Florida, Gainesville, Florida 32611

Rohit Khanna, Kristen Bevlin, and Dwarakanath Geerpuram
Plasma-Therm, Saint Petersburg, Florida 33716

Li-Chun Tung, Jingyu Lin, and Hongxing Jiang
Department of Electrical and Computer Engineering, Texas Tech. University, Lubbock, Texas 79409

Jonathan Lee, Elena Flitsiyan, and Leonid Chernyak
Department of Physics, University of Central Florida, Orlando, Florida 32816

S. J. Pearton[a)]
Department of Materials Science and Engineering, University of Florida, Gainesville, Florida 32611

Akito Kuramata
Tamura Corporation and Novel Crystal Technology, Inc., Sayama, Saitama 350-1328, Japan

The surface of single-crystal (-201) oriented β-Ga$_2$O$_3$ was etched in BCl$_3$/Ar inductively coupled plasmas under conditions (an excitation frequency of 13.56 MHz, a source power of 400 W, and a dc self-bias of -450 V) that produce removal rates of ~700 Å min^{-1}. Annealing at 400 and 450 °C was carried out after etching on Ni/Au Schottky diodes formed on the surface either before or after the annealing step. Current–voltage (I–V) measurements were used to extract the Schottky barrier height (Φ), diode ideality factor (n), and reverse breakdown voltage (V$_{RB}$) for plasma damaged diodes after annealing. Annealing at 450 °C was found to essentially restore the values of Φ, n, and V$_{RB}$ to their reference (unetched) values on samples metallized after etching and annealing. Thermal annealing at either temperature of metallized diodes degraded their reverse breakdown voltage, showing that Ni/Au is not stable on β-Ga$_2$O$_3$ at these temperatures. Photoluminescence revealed a decrease in total emission intensity in the near band-edge region after the introduction of etch damage. Electron beam-induced current measurements showed a decrease in the minority carrier diffusion length from 350 μm in the control sample to 311 μm in the etched sample. © 2017 American Vacuum Society. [http://dx.doi.org/10.1116/1.4986300]

I. INTRODUCTION

β-Ga$_2$O$_3$ is gaining attention for its potential in high breakdown electronics.[1–7] β-polytypes are air-stable, have a wide bandgap (~4.6 eV), and are available as both bulk crystals and epitaxial films.[1–19] Different types of power diodes and transistors fabricated on bulk and epi Ga$_2$O$_3$ have shown impressive performance.[5,6,8–17,19] Although β-Ga$_2$O$_3$ is not a van der Waals 2D material, the monoclinic structure of bulk β-Ga$_2$O$_3$ crystals allows relatively simple cleavage into ultra-thin flakes in the (100) direction and a range of transistor structures have also been demonstrated on what are generally termed nanobelts.[7,18] Etching processes for Ga$_2$O$_3$ are needed for patterning for mesa isolation, threshold adjustment in transistors, thinning of nanobelts, and selective area contact formation. There have been a few studies of wet etching of Ga$_2$O$_3$, where it was found that HNO$_3$ at elevated temperature and hydrofluoric acid at room temperature provide the fastest removal rates.[20,21] Dry etching is preferable because of its higher resolution, and control and initial studies of reactive ion etching (RIE) and inductively coupled plasma (ICP) etching in predominantly chlorine or boron trichloride (Cl$_2$, BCl$_3$) plasma chemistries have shown removal rates up to ~1500 Å min^{-1}

under high power conditions.[22–26] The presence of electrical damage in the near-surface region of ICP etched Ga$_2$O$_3$ was found through barrier height changes of Schottky diodes fabricated on the etched surface.[25,26] The damage is created by energetic ion bombardment but in some cases may also consist of changes to near-surface stoichiometry through the preferential loss of one of the lattice elements or deposition of etch residues. The removal of this damage is key in achieving the best performance of devices patterned by dry etching.

In this paper, we report on the effect of annealing on dry etch damage removal in Ga$_2$O$_3$ diodes formed on surfaces exposed to BCl$_3$/Ar, monitored through the effects on the barrier height, reverse breakdown voltage, minority carrier diffusion length, and ideality factor of Schottky diodes deposited onto the etched surface of Ga$_2$O$_3$ either prior to or subsequent to annealing. This allowed us to determine the thermal stability of both the etch damage and the Schottky metallization. Ni/Au is not stable on Ga$_2$O$_3$ for the 450 °C anneals needed to remove the dry etch damage. We also examined the surfaces by photoluminescence (PL) before and after the dry etching.

II. EXPERIMENT

All experiments were performed with bulk β-phase (−201) oriented Ga$_2$O$_3$ single crystals (Tamura Corporation,

a)Electronic mail: spear@mse.ufl.edu

Japan) grown by the edge-defined film-fed growth method. Hall effect measurements showed that the sample was unintentionally n-type with an electron concentration of $\sim 3 \times 10^{17}\,cm^{-3}$. Full-area back Ohmic contacts were created using Ti/Au (20 nm/80 nm) deposited by e-beam evaporation. Linear current–voltage behavior was obtained without the need for a rapid annealing step. Unmasked samples were exposed to $15BCl_3/5Ar$ discharges (where the numbers represent the respective gas flows in standard cubic centimeters per minute) in a Plasma-Therm Versaline ICP reactor. The 2 MHz power applied to the three-turn ICP source was 400 W, while the rf (13.56 MHz) chuck power was 200 W. The dc self-bias on the sample electrode was $\sim 450\,V$. The Ga_2O_3 etch rate under these conditions is $\sim 700\,\text{Å}\,min^{-1}$, and the samples were etched for 3 min.

A schematic of the experimental sequence is shown in Fig. 1. Schottky contacts were prepared on the front sides of the samples after etching by e-beam deposition of Ni/Au (20 nm/80 nm) contacts through a stencil mask. In some cases, the samples were annealed at 400 or 450 °C for 10 min in an Ar ambient prior to Schottky deposition, while other diodes were annealed after the contacts were deposited. This enabled us to check both the removal of dry etch damage and the thermal stability of the Ni/Au metallization on Ga_2O_3 and is relevant for determining the process sequence after dry etching. The forward and reverse current–voltage (I–V) characteristics were recorded at 25 °C using an Agilent 4145B parameter analyzer.[27] The basic current transport processes in Schottky contacts on moderately doped samples like these will be thermionic emission.[28–30] The I–V characteristic is then given by the relation[28]

$$ I = I_S \exp\left(eV/n\text{kT}\right)\left[1 - \exp\left(-\frac{eV}{n\text{kT}}\right)\right], $$

where I_S is the saturation current given by

$$ I_S = AA*T^2 \exp(\varphi_b)/\text{kT}, $$

A is the contact area, A^* is the effective Richardson constant ($33.7\,A\,cm^{-2}\,K^{-2}$ for Ga_2O_3), Φ_B is the effective barrier

height, n is the ideality factor, e is the electronic charge, k is Boltzmann's constant, and T is the absolute temperature. For extraction of the effective barrier height from the I–V characteristics of our Schottky diodes, we fitted the linear portions that obeyed the ideal thermionic-emission behavior. The ideality factor n should be close to unity, with a small increase due to the image force effect.[28–30]

The same diode structures were used to carry out minority carrier diffusion length measurements by recording the exponential decay of electron beam-induced current as a function of the distance from the gate. The surface recombination velocity, v_s, was assumed to be negligible (i.e., $v_s \simeq 0$; $\alpha = -0.5$). Each diffusion length determined was an average of a minimum of seven measurements. The diffusion length was found using[31–33]

$$ I(x) = I_0 x^a \exp[-x/L], $$

where $I(x)$ is the electron beam-induced current (EBIC) signal intensity as a function of distance, I_0 is the intensity at the contact edge, x is the beam-to-junction distance, and L is the diffusion length. Coefficient α is related to the surface recombination velocity, v_s, and is taken to be equal to $-1/2$. The diffusion length can be directly extracted from the above relationship. All the measurements on the devices were performed *in situ* in a Philips XL 30 scanning electron microscope (SEM) under an accelerating voltage of 16 kV. EBIC data were acquired by scanning the electron beam of the SEM along a line perpendicular to the edge of gate contacts and recording the exponential decay of the current.

PL spectra at 10 K were measured in a SHI-APD closed-cycle optical cryostat using an ARC AM-511 Czerny-Turner 1.3 m monochromator with a 1800 grooves/mm grating. An excimer laser provides an intensive pumping light source (100 mJ per pulse, 15 ns duration, and 20 Hz repetition rate) of 193 nm (6.42 eV), and a photomultiplier tube is attached to the outside slit of the monochromator for optical detection. The output of the photomultiplier tube is amplified and fed to an ORTEC 661 ratemeter, and so, the rate of photons arriving at the slit is measured. As a result, the magnitude of the photoluminescence spectra reflects the number of emitted photons at a given energy per unit time. The samples were placed side-by-side inside a closed-cycle He refrigerator.

III. RESULTS AND DISCUSSION

Three diodes were measured for each condition, and the results were found to be within 5% in terms of breakdown voltage. Schottky diode measurements are effective monitors of ion-induced damage in semiconductors[34–37] and have been used extensively for GaN (Refs. 34 and 35) and monitoring of irradiation damage in Ga_2O_3.[25] The unetched diodes showed barrier heights of 1.08 eV and ideality factors of 1.12, consistent with previous reports for Ni on Ga_2O_3.[27,29,30,36]

Figure 2 shows the forward I–V characteristics of the reference, plasma exposed, and samples annealed at either 400 or 450 °C after etching and then deposited with the Ni/Au contacts. As shown in Table I, the introduction of the etch damage decreased the barrier height (0.85 eV) and increased the ideality factor (1.33). This is similar to the trends
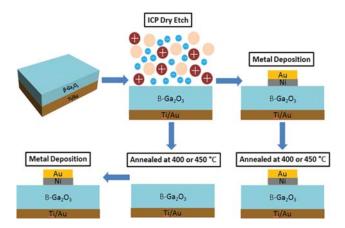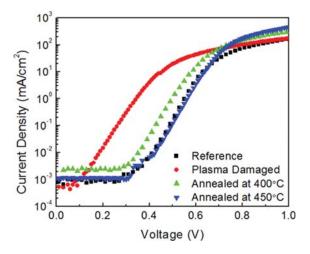
FIG. 1. (Color online) Schematic of experiment-Ni/Au Schottky diodes formed on dry etched β-Ga_2O_3 surfaces either before or after subsequent annealing at 400 or 450 °C.

FIG. 2. (Color online) Forward I–V characteristics of Ni/Au Ga$_2$O$_3$ diodes on surfaces dry etched in BCl$_3$/Ar ICP discharges and annealed at 400 or 450 °C prior to metallization.

FIG. 3. (Color online) Reverse I–V characteristics of Ni/Au Ga$_2$O$_3$ diodes on surfaces dry etched in BCl$_3$/Ar ICP discharges and annealed at 400 °C either before or after deposition of Ni/Au.

reported previously for ICP etching of both GaN (Refs. 34 and 35 and ZnO.[37] Annealing at 400 °C improved both parameters, while annealing at 450 °C essentially restored the predamage values ($\Phi_B = 1.09$ eV and n = 1.14). This is a significantly lower temperature than that required for the removal of dry etch damage in GaN,[36] where annealing temperatures of 700–800 °C produced a recovery of only ~70% of the degraded electrical properties. In that case, immersion in hot potassium hydroxide was required to remove the damaged GaN and restore the properties of the surface.[36] This is not applicable to Ga$_2$O$_3$ because our preliminary results show uncontrollably high removal rates under these conditions.

Figure 3 shows the reverse I–V characteristics of the diodes before and after etch damage introduction and after annealing at 400 °C. There are a number of points obvious from the data. First, the reverse breakdown voltage is decreased. These etch rate conditions with a high source and chuck power lead to a decrease in breakdown voltage of ~64%. The degradation in reverse characteristics is common in dry etched semiconductors and is ascribed to the introduction of point defects that act as generation-recombination centers and traps for free carriers.[34,35] Second, annealing at 400 °C only partially restores the reverse characteristics. Third, annealing with Ni/Au in place severely degrades (~75% reduction) the reverse breakdown voltage, even on the reference sample that was not exposed to a plasma. This shows that Ni/Au has limited thermal stability on Ga$_2$O$_3$, which has implications for the stability of Schottky rectifiers

on this material at elevated operating temperatures and also points to the fact that annealing to remove etch damage has to be done prior to subsequent metallization. Other choices for the Schottky contact might display superior thermal stability on Ga$_2$O$_3$.

Figure 4 shows similar reverse I–V characteristics for the same etching conditions as Fig. 3, but for annealing at 450 °C. The same trends are evident, but the reverse breakdown voltage is almost completely restored by the 450 °C anneal when Ni/Au is deposited after this anneal. This shows that relatively low temperature anneals are sufficient to remove ICP etch damage in Ga$_2$O$_3$, which enhances the attractiveness of this technique for patterning of device structures.

PL spectroscopy was employed as a nondestructive method for characterizing the emission properties of reference and plasma damaged Ga$_2$O$_3$ samples. The bandgap was found to be ~4.9 eV.[38,39] As shown in Fig. 5(a), optical

TABLE I. Schottky barrier height and diode ideality factor for Ga$_2$O$_3$ before and after ICP etching in 15 BCl$_3$/5 Ar discharges and subsequent annealing.

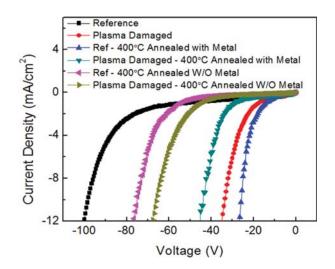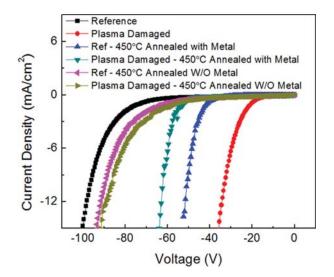| Sample	Reverse breakdown voltage (V)	Schottky barrier height (eV)	Ideality factor
Reference	-100 ± 5	1.08	1.12
Plasma damaged	-36 ± 3	0.85	1.33
Annealed at 400 °C	-67 ± 4	1.00	1.23
Annealed at 450 °C	-91 ± 5	1.09	1.14

FIG. 4. (Color online) Reverse I–V characteristics of Ni/Au Ga$_2$O$_3$ diodes on surfaces dry etched in BCl$_3$/Ar ICP discharges and annealed at 450 °C either before or after deposition of Ni/Au.
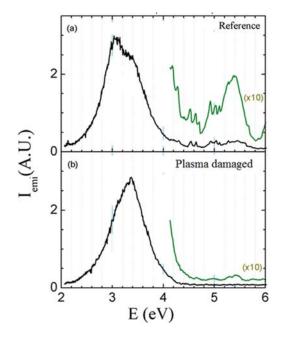
FIG. 5. (Color online) Comparison of 10 K photoluminescence of spectra of (a) a reference Ga_2O_3 sample and (b) a plasma damaged Ga_2O_3 sample. The higher energy peaks exhibit the spectra measured in the higher sensitivity range and are enlarged for clarity.

transitions from the O defect donor band to the valence band ($E_{DB} = 3.411$ eV) and to the Ga vacancy band ($E_{D2} = 3.002$ eV to $E_{D3} = 2.39$ eV)[38] dominate the photoluminescence spectrum of the reference sample. This midgap emission is much larger than the bandedge emission. Dong et al.[38,40] found that oxygen vacancies can induce additional emission peaks in the PL spectrum. There are three types of O sites in β-Ga_2O_3.[40] As a result, three types of neutral oxygen vacancies exist, denoted as V_{OI}, V_{OII} (both are threefold coordinated), and V_{OIII} (fourfold coordinated), respectively, in the work by Dong et al.[40] They predict using density functional calculations that oxygen vacancies can induce absorption peaks at 3.80, 3.52, and 3.37 eV for V_{OI}, V_{OII}, and V_{OIII}, respectively. Some of these centers may contribute to the broad defect peak in our samples between 3 and 4 eV. ICP damage results in a change in the ratio of O-related defects to Ga vacancies and thus a change in the photoluminescence signal corresponding to the optical transitions from the defect donor band to the Ga vacancy band. The near bandedge region around 4.9 eV shows a decrease in total intensity in the etch damaged sample. However, the overall changes in defect bands are difficult to quantify and relate to the fact that the sampling depth of PL ($\sim 1\ \mu$m) is large compared to the expected damaged region thickness of <1000 Å. In addition, there is interference from laser lines beyond the actual bandedge of Ga_2O_3.

EBIC measurements determined the minority carrier diffusion length in the control sample to be $L = 350 \pm 75$ nm. In the plasma damaged sample, there was a reduction in this value of $\sim 11\%$, i.e., the minority carrier diffusion length was $L = 307 \pm 43$ nm. For all measurements, the accelerating voltage was 16 kV. This corresponds to a range of ~ 1

um. Since this is similar to the sampling depth of the PL, this shows that the minority carrier diffusion length is still sensitive to changes in the near-surface crystal order.

What is the expected nature of the etch-induced defects? Previous reports have shown that the O/Ga ratio near the surface does not change within the detectable sensitivity of Auger Electron Spectroscopy measurements.[36] Varley et al.[41] have suggested using density functional theory calculations that oxygen vacancies are deep donors and do not explain the native n-type conductivity in Ga_2O_3. Ma et al.[42] found a similar result. Dong et al.[43] found that N acceptors and native defects such as Ga and O interstitials and vacancies can create various compensation effects. Son et al.[44] suggested that the dominant donor is Si. Kananen et al.[45] identified doubly and singly ionized Ga vacancies in neutron-irradiated Ga_2O_3 using electron paramagnetic resonance, but these are acceptors. Wendler et al.[46] found predominantly point defects created during subamorphizing ion implantation into Ga_2O_3. As-grown Ga_2O_3 is found to have a large number of defect states distributed throughout the bandgap.[47] All this suggests that simple creation of oxygen vacancies might not be the cause of the degradation in barrier properties as a result of the introduction of dry etch damage although these acting as recombination centers can explain the change in diode characteristics.

IV. SUMMARY AND CONCLUSIONS

In summary, ion-assisted dry etching processes for Ga_2O_3 create near-surface damage which can be removed by annealing at 450 °C. This treatment is sufficient to essentially fully restore both the forward and reverse I–V characteristics of diodes fabricated on these surfaces. The thermal stability of Ni/Au rectifying contacts on Ga_2O_3 is insufficient to stand this temperature, and the contacts need to be deposited after the anneal step. The minority carrier diffusion length is degraded in the etched samples.

ACKNOWLEDGMENTS

[1] M. A. Mastro, A. Kuramata, J. Calkins, J. Kim, F. Ren, and S. J. Pearton, ECS J. Solid State Sci. Technol. **6**, P356 (2017).
[2] S. I. Stepanov, V. I. Nikolaev, V. E. Bougrov, and A. E. Romanov, Rev. Adv. Mater. Sci. **44**, 63 (2016), available at http://www.ipme.ru/e-journals/RAMS/no_14416/06_14416_stepanov.pdf.
[3] M. J. Tadjer et al., J. Electron. Mater. **45**, 2031 (2016).

[4]E. G. Villora, S. Arjoca, K. Shimamura, D. Inomata, and K. Aoki, Proc. SPIE **8987**, 89871U (2014).

[5]O. Ueda, N. Ikenaga, K. Koshi, K. Iizuka, A. Kuramata, K. Hanada, T. Moribayashi, S. Yamakoshi, and M. Kasu, Jpn. J. Appl. Phys., Part 1 **55**, 1202BD (2016).

[6]M. J. Tadjer, N. A. Mahadik, V. D. Wheeler, E. R. Glaser, L. Ruppalt, A. D. Koehler, K. D. Hobart, C. R. Eddy, Jr., and F. J. Kub, ECS J. Solid State Sci. Technol. **5**, 468 (2016).

[7]J. Kim, S. Oh, M. Mastro, and J. Kim, Phys. Chem. Chem Phys. **18**, 15760 (2016).

[8]N. A. Moser, J. P. McCandless, A. Crespo, K. D. Leedy, A. J. Green, E. R. Heller, K. D. Chabak, N. Peixoto, and G. H. Jessen, Appl. Phys. Lett. **110**, 143505 (2017).

[9]S. Rafique, L. Han, M. J. Tadjer, J. A. Freitas, Jr., N. A. Mahadik, and H. Zhao, Appl. Phys. Lett. **108**, 182105 (2016).

[10]M. Higashiwaki, K. Sasaki, H. Murakami, Y. Kumagai, A. Koukitu, A. Kuramata, T. Masui, and S. Yamakosh, Semicond. Sci. Technol. **31**, 034001 (2016).

[11]K. D. Chabak *et al.*, Appl. Phys. Lett. **109**, 213501 (2016).

[12]A. J. Green *et al.*, IEEE Electron Device Lett. **37**, 902 (2016).

[13]H. Zhou, M. Shi, S. Alghamdi, G. Qui, L. Yang, and P. Ye, IEEE Electron Device Lett. **38**, 103 (2017).

[14]J. Yang, S. Ahn, F. Ren, S. J. Pearton, S. Jang, J. Kim, and A. Kuramata, Appl. Phys. Lett. **110**, 192101 (2017).

[15]M. H. Wong, Y. Nakata, A. Kuramata, S. Yamakoshi, and M. Higashiwaki, Appl. Phys. Express **10**, 041101 (2017).

[16]S. Oh, G. Yang, and J. Kim, ECS J. Solid State Sci. Technol. **6**, Q3022 (2017).

[17]K. Konishi, K. Goto, H. Murakami, Y. Kumagai, A. Kuramata, S. S. Yamakoshi, and M. Highisiwaki, Appl. Phys. Lett. **110**, 103506 (2017).

[18]S. Ahn, F. Ren, J. Kim, S. Oh, J. Kim, M. A. Mastro, and S. J. Pearton, Appl. Phys. Lett. **109**, 062102 (2016).

[19]K. Zheng, J. S. Wallace, C. Hemiburger, K. Sasaki, A. Kuramata, T. Masui, J. S. Gardella, and U. Singisetti, IEEE Electron Device Lett. **38**, 513 (2017).

[20]S. Ohira and N. Arai, Phys. Status Solidi C **5**, 3116 (2008).

[21]H. Liang, Y. Chen, X. Xia, C. Zhang, R. Shen, Y. Liu, Y. Luo, and G. Du, Mater. Sci. Semicond. Process. **39**, 582 (2015).

[22]J. E. Hogan, S. W. Kaun, E. Ahmadi, Y. Oshima, and J. S. Speck, Semicond. Sci. Technol. **31**, 065006 (2016).

[23]A. P. Shah and A. Bhattacharya, J. Vac. Sci. Technol., B. **35**, 041301 (2017).

[24]J. Yang, S. Ahn, F. Ren, R. Khanna, K. Bevlin, D. Geerpuram, S. J. Pearton, and A. Kuramata, Appl. Phys. Lett. **110**, 142101 (2017).

[25]J. Yang, S. Ahn, F. Ren, S. J. Pearton, R. Khanna, K. Bevlin, D. Geerpuram, and A. Kuramata, J. Vac. Sci. Technol., B **35**, 031205 (2017).

[26]Y. Kwon, G. Lee, S. Oh, J. Kim, S. J. Pearton, and F. Ren, Appl. Phys. Lett. **110**, 131901 (2017).

[27]S. Ahn, F. Ren, L. Yuan, S. J. Pearton, and A. Kuramata, ECS J. Solid State Sci. Technol. **6**, P68 (2017).

[28]S. M. Sze and K. K. Ng, *Physics of Semiconductor Devices*, 3rd ed. (Wiley, Hoboken, 2007), Chap. 3.

[29]T. Oishi, Y. Koga, K. Harada, and M. Kasu, Appl. Phys. Express **8**, 0311019 (2015).

[30]Y. Yao, R. Gangireddy, J. Kim, K. K. Das, R. F. Davis, and L. M. Porter, J. Vac. Sci. Technol., B **35**, 03D113 (2017).

[31]C. Schwarz *et al.*, Appl. Phys. Lett. **102**, 062102 (2013).

[32]D. E. Ioannou and C. A. Dimitriadis, IEEE Trans. Electron Devices **29**, 445 (1982).

[33]J. Boersma, J. J. E. Lindenkleef, and H. K. Kuiken, J. Eng. Math. **18**, 315 (1984).

[34]X. Cao *et al.*, Appl. Phys. Lett. **75**, 232 (1999).

[35]X. A. Cao, S. J. Pearton, G. T. Dang, A. P. Zhang, F. Ren, and J. M. Van Hove, IEEE Trans. Electron Devices **47**,1320 (2000).

[36]J. Yang, F. Ren, S. J. Pearton, G. Yang, J. Kim, and A. Kuramata, J. Vac. Sci. Technol., B **35**, 031208 (2017).

[37]K. Ip, K. Baik, M. E. Overberg, E. S. Lambers, Y. W. Heo, D. P. Norton, S. J. Pearton, F. Ren, and J. M. Zavada, Appl. Phys. Lett. **81**, 3546 (2002).

[38]C.-H. Ho, C.-Y. Tseng, and L.-C. Tien, Opt. Express **18**, 16360 (2010).

[39]S. Fujita, Jpn. J. Appl. Phys. **54**, 030101 (2015).

[40]L. Dong, R. Jia, B. Xin, B. Peng, and Y. Zhang, Sci. Rep. **7**, 40160 (2017).

[41]J. B. Varley, J. R. Weber, A. Janotti, and C. G. Van de Walle, Appl. Phys. Lett. **97**, 142106 (2010).

[42]X. Ma, Y. Zhang, L. Dong, and R. Jia, Results Phys. **7**, 1582 (2017).

[43]L. Dong, R. Jia, C. Li, B. Xin, and Y. Zhang, J. Alloys Compd. **712**, 379 (2017).

[44]N. T. Son *et al.*, J. Appl. Phys. **120**, 235703 (2016).

[45]B. E. Kananen, L. E. Halliburton, K. T. Stevens, G. K. Foundos, and N. C. Giles, Appl. Phys. Lett. **110**, 202104 (2017).

[46]E. Wendler, E. Treiber, J. Baldauf, S. Wolf, and C. Ronnig, Nucl. Instrum. Methods Phys. Res., B **379**, 85 (2016).

[47]Z. Zhang, E. Farzana, A. R. Arehart, and S. A. Ringel, Appl. Phys. Lett. **108**, 052105 (2016).